J Sol-Gel Sci Technol (2015) 76:98–109
DOI 10.1007/s10971-015-3756-7

ORIGINAL PAPER

Preparation of poly(aryl ether ketone ketone)–silica composite aerogel for thermal insulation application

Xueliang Pei[1] · **Wentao Zhai**[1] · **Wenge Zheng**[1]

Received: 13 March 2015 / Accepted: 21 May 2015 / Published online: 3 June 2015

Abstract In this study, poly(aryl ether ketone ketone) (PEKK) with trimethoxysilane pendant groups was prepared first and then chemically cross-linked PEKK–silica composite wet gel was formed through the hydrolysis and condensation reactions of the trimethoxysilane pendant groups at room temperature. ^{29}Si solid-state nuclear magnetic resonance indicated that 70.5 % of the methoxy groups on silicon participated in the condensation reaction. The formed PEKK–silica composite wet gel was dried by freeze-drying from *tert*-butanol to obtain PEKK–silica composite aerogel, which consisted of polymer fibers tangled together. By adjusting the concentration of PEKK with trimethoxysilane pendant groups in solution, PEKK–silica composite aerogels with different densities (ranging from 0.17 to 0.40 g/cm^3) were obtained. The resulting aerogels had small average pore diameters (ranging from 25.0 to 59.4 nm), high surface areas (ranging from 299 to 354 m^2/g), low thermal conductivities (ranging from 0.024 to 0.035 W/m K at room temperature) and good mechanical property. Although PEKK lost crystallization ability after incorporating trimethoxysilane pendant groups, the cross-linked PEKK still had a storage modulus as high as 1026 MPa at 300 °C. So, even after being heated at 250 °C for 30 min in air, the pore structure of PEKK–silica composite aerogel was still intact.

Graphical Abstract

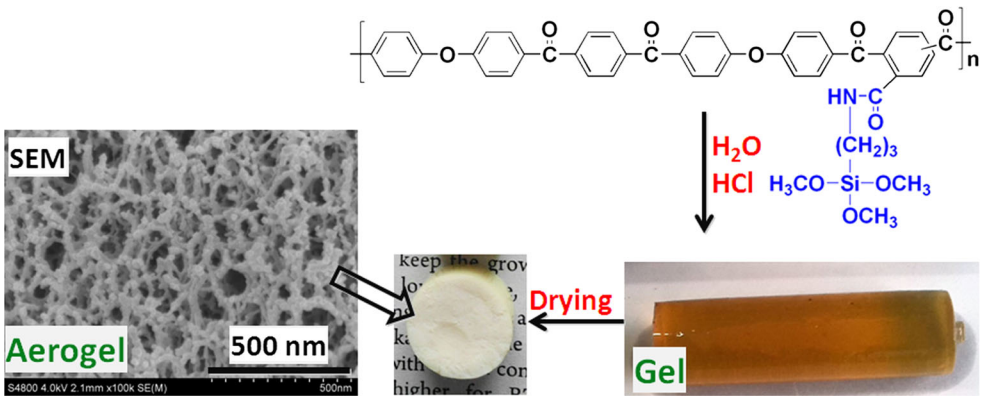

Keywords Poly(aryl ether ketone ketone) · Aerogel · Thermal conductivity · Thermal stability

✉ Xueliang Pei
peixueliang@nimte.ac.cn

✉ Wenge Zheng
wgzheng@nimte.ac.cn

[1] Polymers and Composites Division, Ningbo Institute of Material Technology and Engineering, Chinese Academy of Sciences, Ningbo 315201, Zhejiang, People's Republic of China

1 Introduction

At present, consumption of fuels is growing dramatically in response to increasing population, improvement in quality of life and rapid industrialization of the world. However, excessive fuel consumption not only leads to a significant decrease in fuel reserves, but also causes problems threatening public health and environment. Improving energy use efficiency is an effective way for reducing fuel consumption, and it has long been recognized that using thermal insulation materials is a good method of accomplishing this goal.

Generally, heat is transferred by conduction, convection and radiation [1]. Aerogel is a lightweight open-celled mesoporous material, which is typically prepared by forming a wet gel that includes three-dimensional skeleton network and a liquid component first and then removing the liquid component inside without causing collapse of the three-dimensional skeleton network [2]. The low density and three-dimensional skeleton network of aerogel provide tortuous and limited pathways for heat transfer via solid. In addition, most or all pores in aerogel are classified as mesopores sized between 2 and 50 nm, namely below the mean free path of air molecules ($\sim$70 nm), so the heat transfer via gas within the aerogel is suppressed. Therefore, aerogel offers a distinct advantage over conventional thermal insulation materials and exhibits the lowest thermal conductivity of any of the solids or porous materials [3–6]. For example, for silica aerogel with a density of 0.150 g/cm^3, the thermal conductivity at room temperature was 0.015 W/m K [7]. The thermal conductivity of resorcinol–formaldehyde aerogel has been measured by Lu et al. [8] as a function of density, and a record-low conductivity value (0.012 W/m K) at room temperature was found for 0.157 g/cm^3. Guo et al. [9] prepared polyimide aerogel having a density around 0.1 g/cm^3 from 3,3′,4,4′-biphenyltetracarboxylic dianhydride, bisaniline-*p*-xylidene and octa-(aminophenyl) silsesquioxane, and the polyimide aerogel had ambient thermal conductivity of 0.015 W/m K. In contrast, the ambient thermal conductivities of conventional thermal insulation materials like mineral wool, glass wool, foam glass and expanded polystyrene were in the range of 0.029–0.055 W/m K [1]. This is the reason why the aerogel has a tremendous annual growth rates from 50 to 75 % in recent years, and similar developments are expected for the near future [6].

In the latest 30 years, there have been many investigations of the application of aerogel to the field of thermal insulation. Among various aerogels, silica aerogel is the most well-known and extensively studied. Its excellent transparency makes it a promising material for window insulation and solar tank [10, 11]. However, the pure silica aerogel is extremely fragile (low strength and high brittleness) because of the weak linkages in its 'pearl-necklace-like' three-dimensional network structure [12, 13]. To overcome the drawbacks associated with the weakness and brittleness of silica aerogel, various strategies have been investigated, most notably via cross-linking of its skeletal framework with polymers or molecules possessing two or more reactive groups and reinforcing with fibers [14–17]. Fiber reinforcements improve the mechanical property of silica aerogel significantly, and fiber-reinforced silica aerogel composites have been commercialized, but they are still dusty due to the inherent brittleness of silica aerogel [18]. In addition, the incorporation of fibers could reduce the transparency of silica aerogel [14].

Compared with the pure silica aerogel, organic aerogels exhibit much better mechanical property [19–24]. Poly(aryl ether ketone)s are high-performance polymers possessing high thermal stability and good mechanical property, which have received commercial and industrial interest. In addition, inspired by the fact that alkoxysilanes have high hydrolysis and condensation reactivity, trimethoxysilane pendant groups were incorporated into the poly(aryl ether ketone ketone) (PEKK) chain and chemically cross-linked PEKK–silica composite aerogel was formed through the hydrolysis and condensation reactions of the trimethoxysilane pendant groups in this study. The structure, morphology, mechanical property, thermal stability and thermal conductivity of the resulting PEKK–silica composite aerogel were characterized.

2 Experimental section

2.1 Materials

1,4-Bis(4-phenoxybenzoyl) benzene was synthesized as reported in the literature [25]. Trimellitic anhydride acid chloride was purified by sublimation in vacuum. *N*,*N*′-dimethylformamide (DMF) and 1,2-dichloroethane (DCE) were distilled over phosphorus pentoxide and stored over 4 Å molecular sieves. 3-Aminopropyltrimethoxysilane, *N*-methyl-2-pyrrolidone, triethylamine, thionyl chloride and *tert*-butanol were purchased from Sinopharm Chemical Reagent and used as received without further purification.

2.2 Synthesis of PEKK with carboxylic acid pendant groups

Anhydrous $AlCl_3$ powder (32.0 g, 240 mmol) and DCE (60 mL) were added into a 250-mL three-necked round-bottomed flask equipped with a mechanical stirrer. After stirring at room temperature for 30 min, the flask was cooled

to 0 °C and *N*-methyl-2-pyrrolidone (7.4 g, 75 mmol) in DCE (30 mL) was added dropwise with stirring under nitrogen atmosphere. Most of $AlCl_3$ was dissolved after the addition of *N*-methyl-2-pyrrolidone. Then, the flask was cooled to −20 °C followed by addition of 1,4-bis(4-phenoxybenzoyl) benzene (11.5275 g, 24.5 mmol) and trimellitic anhydride acid chloride (5.2643 g, 25 mmol). The reaction mixture was allowed to react at −20 °C for 2 h and at room temperature for 8 h. After that, the reaction was quenched by careful addition of diluted hydrochloric acid to afford a white precipitate. The resulting white precipitate was crushed, washed with water, extracted with boiling ethanol for 24 h and dried under vacuum at 120 °C for 12 h.

2.3 Synthesis of PEKK with trimethoxysilane pendant groups

PEKK with carboxylic acid pendant groups (0.6446 g, the molar content of carboxylic acid pendant group was 1 mmol), thionyl chloride (5 mL) and two drops of DMF were added into a 50-mL round-bottomed flask. The mixture was heated to 85 °C and stirred at the temperature for 0.5 h. Most of excess thionyl chloride was removed by distillation under normal pressure, and then distillation at 140 °C under vacuum for 1 h was carried out to eliminate any residual thionylchloride. After cooling to room temperature, 3-aminopropyltrimethoxysilane (0.1793 g, 1 mmol), triethylamine (0.1012 g, 1 mmol) and DMF (8 mL) were added to the flask. The reaction mixture was stirred at room temperature for 2 h, and then, the precipitated triethylamine hydrochloride was removed by filtration. The obtained DMF solution of PEEK with trimethoxysilane pendant groups would be used in the next step directly without any additional purification.

2.4 Preparation of PEKK–silica composite aerogel

As shown in Table 1, three PEKK–silica composite aerogels with different densities were prepared. The preparation of Sample 1 is used below as an example to illustrate the preparation route. A solution of water (0.0900 g, 5 mmol) and HCl (0.0037 g, 0.10 mmol) in DMF (12 mL) was added into the obtained DMF solution of PEKK with trimethoxysilane pendant groups. After vigorous stirring for 3 min, the reaction mixture was drawn into syringes. A wet gel formed within 1 h, and the wet gel was allowed to age in the syringes for 3 days at room temperature. After the aging treatment, the resulting wet gel was removed from the syringes, and the solvent within the wet gel was exchanged with *tert*-butanol (4 times, at 40 °C for 12 h each time). Then, the wet gel containing *tert*-butanol was frozen at −25 °C overnight, followed by freeze-drying at −25 °C under vacuum condition to afford the PEKK–silica composite aerogel. By varying the concentration of PEKK with trimethoxysilane pendant groups in DMF, PEKK–silica composite aerogels with different densities were obtained.

2.5 Characterization

The inherent viscosity was measured at 30 ± 0.1 °C in DMF with an Ubbelohde viscometer, and the concentration was 0.5 g/dL. Fourier transform infrared (FTIR) spectra were recorded with a Thermo Nicolet 6700 FTIR spectrometer (available from Thermo Nicolet Corp, USA), and the samples were prepared with KBr pellets. ^{29}Si solid-state nuclear magnetic resonance (^{29}Si NMR) spectrum was recorded on a Bruker AVANCE III 400 spectrometer (available from Bruker Corp, Switzerland) at a resonance frequency of 79.30 MHz. Bulk densities of aerogels were determined by weighing the sample and dividing the weight by its measured geometrical volume. Skeletal densities of aerogels were obtained from a Micromeritics Accupyc 1340 helium pycnometer (available from Micromeritics Instrument Corp, Germany). Rheological measurement was carried out on a rotational Physica MCR 301 rheometer (available from Anton Paar Corp, Austria). The complex viscosity, storage modulus (G′) and loss modulus (G″) data were isothermally collected at 25 °C with a sweep frequency of 1 Hz and a strain amplitude of 1 % (well inside the linear viscoelastic range). Dynamic mechanical thermal analysis (DMTA) was conducted with a Mettler Toledo DMA (available from Mettler Toledo

Table 1 Densities and shrinkages during preparation of PEKK–silica composite aerogels

Sample	Solid content (g/mL)[a]	Density (g/cm^3)[b]	Shrinkage (%)[c]		
			During aging	During solvent exchange	During freeze-drying
Sample 1	0.04	0.18 ± 0.01	13	19	8
Sample 2	0.05	0.25 ± 0.02	21	15	6
Sample 3	0.06	0.38 ± 0.02	26	13	5

[a] The content of PEKK with trimethoxysilane pendant groups in solution

[b] The density value of the final PEKK–silica composite aerogel

[c] Shrinkage was calculated via 100 × (mold diameter − sample diameter)/(mold diameter)

Corp, Switzerland) in a load frequency of 1 Hz and a tensile mode at a heating rate of 5 °C/min under air atmosphere. Thermogravimetric analysis (TGA) was performed on a Mettler Toledo-TGA/DSC I instrument (available from Mettler Toledo Corp, Switzerland) at a heating rate of 10 °C/min from 50 to 800 °C under air atmosphere (flow rate of 50 mL/min). Morphology of aerogels was performed on a Hitachi S-4800 scanning electron microscope (SEM) (available from Hitachi High-Technologies Corp, Japan). All SEM samples were sputter-coated with gold prior to the observation. Nitrogen adsorption–desorption isotherms were carried out on a Micromeritics ASAP 2020M system (available from Micromeritics Instrument Corp, USA) at liquid nitrogen temperature. Mechanical property under compression was measured by an Instron model 5567 tensile tester (available from Instron Corp, USA). The wide-angle X-ray diffraction (WXRD) measurement was undertaken on a Bruker D8 Advance (available from Bruker Corp, Germany) with Cu Kα radiation (40 kV, 40 mA) at a scanning rate of 5°/min from 5° to 50°. The thermal conductivities of aerogels were measured by Hot Disk TPS 2500S thermal constant analyzer (available from Hot Disk AB, Sweden).

3 Results and discussion

A wet gel consists of a sponge-like, three-dimensional solid network whose pores are usually filled with a liquid [2]. When the liquid in pores is replaced by air without collapsing the pore structure, aerogel is obtained. So the formation of wet gel is a key step in the preparation of aerogel.

In general, polymeric wet gels could be obtained in the following way: (1) crystallization of crystalline polymers in solvents [26–29]; (2) polymerization of multifunctional monomers in solvents [30–32]; (3) cross-linking of linear polymers in solvents [33–35]. PEKK is a semicrystalline polymer, and it also possesses remarkable chemical stability and solvent resistance [36–38]. So, in order to prepare PEKK wet gel, functionalization of PEKK is necessary. Zolotukhin et al. [39] prepared poly(aryl ether ketone)s having carboxylic acid pendant groups by Friedel–Crafts copolycondensation of 4,4′-diphenoxybenzophenone with a mixture of terephthaloyl chloride and trimellitic anhydride acid chloride. In addition, more highly reactive derivatives of carboxylic acid group such as acyl chloride group can be obtained for further chemical transformation. So, in this study, PEKK with trimethoxysilane pendant groups was synthesized by three steps as shown in Scheme 1. Firstly, PEKK with carboxylic acid pendant groups was prepared by the Lewis acid-catalyzed Friedel–Crafts acylation reaction of 1,4-bis(4-phenoxybenzoyl) benzene with trimellitic anhydride acid chloride. The PEKK with carboxylic acid pendant groups had an inherent viscosity of 0.32 dL/g when measured in DMF at a concentration of 0.5 g/dL at 30 °C. It should be noted that, because the configuration of trimellitic anhydride acid chloride is asymmetric, two different types of acylation can occur, affording either *meta*-orientation or *para*-orientation of the resulting two ketone groups. According to the ^{1}H NMR spectrum of the PEKK with carboxylic acid pedant groups shown in Fig. 1, the ratio of *meta*-oriented ketone linkages to *para*-oriented ketone linkages was about 84/16. Then, the carboxylic acid pendant groups of PEKK were converted into acyl chloride pendant groups by reacting with thionyl chloride. The acyl chloride group is highly reactive, which reacted with amino group of 3-aminopropyltrimethoxysilane at room temperature to afford the PEKK with trimethoxysilane pendant groups.

The chemical structure change on the pendant groups of PEKK was confirmed by FTIR spectroscopy. As shown in Fig. 2, C=O stretching absorption peak of the carboxylic acid pendant group was at 1725 cm^{-1}. After treatment with thionyl chloride, the C=O stretching absorption peak of carboxylic acid pendant group nearly disappeared and the C=O stretching absorption peak of acyl chloride pendant group appeared at 1798 cm^{-1} (the absorption peak appeared at 1733 cm^{-1} was due to the hydrolysis of acyl chloride pendant group during FTIR measurement). After reaction with 3-aminopropyltrimethoxysilane, the C=O stretching absorption peak of acyl chloride pendant group disappeared and the C=O stretching absorption peak of amide group was detected at 1707 cm^{-1} as a shoulder peak.

The hydrolysis and condensation reactions of trimethoxysilane pendant groups of PEKK were responsible for the formation of PEKK–silica composite wet gel. The PH value is the decisive parameter for the relative rates of hydrolysis reaction and condensation reaction of alkoxysilanes. Under basic condition, condensation reaction is favored, and hydrolysis is the rate-determining step. In contrast, under acidic condition (pH < 5), condensation reaction is the rate-determining step [2, 40]. Alkoxysilanes with different structures are widely used to prepare SiO_2 aerogels. In order to regulate the rate of hydrolysis and condensation reactions of alkoxysilanes and the microstructure of SiO_2 aerogels, it is highly favorable to run the two-step procedure using an acid catalyst in the first step and a basic catalyst in the second step [2, 40]. However, we found that the two-step procedure was not feasible for PEKK with trimethoxysilane pendant groups. This was because PEKK with trimethoxysilane pendant groups had a high molecular weight and even slight condensation reaction occurred under acidic condition made the viscosity

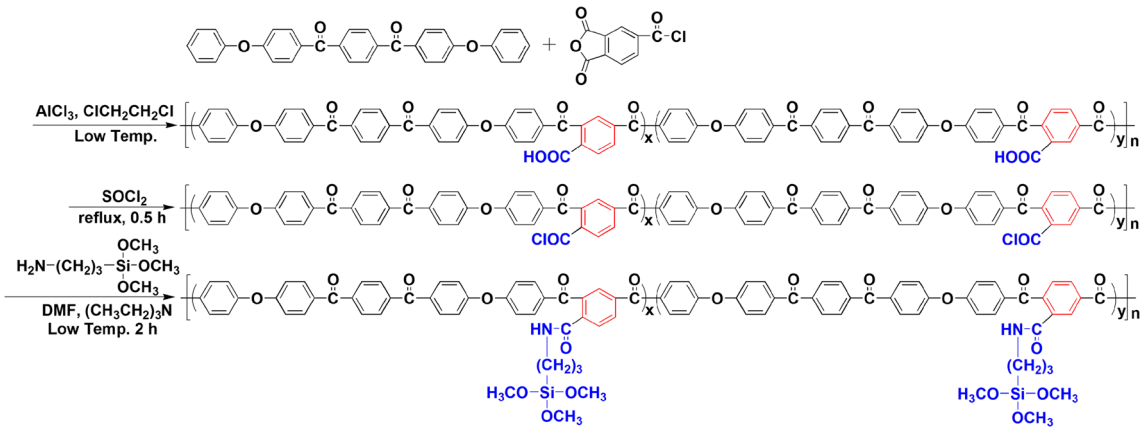

Scheme 1 Synthesis of PEKK with trimethoxysilane pendant groups

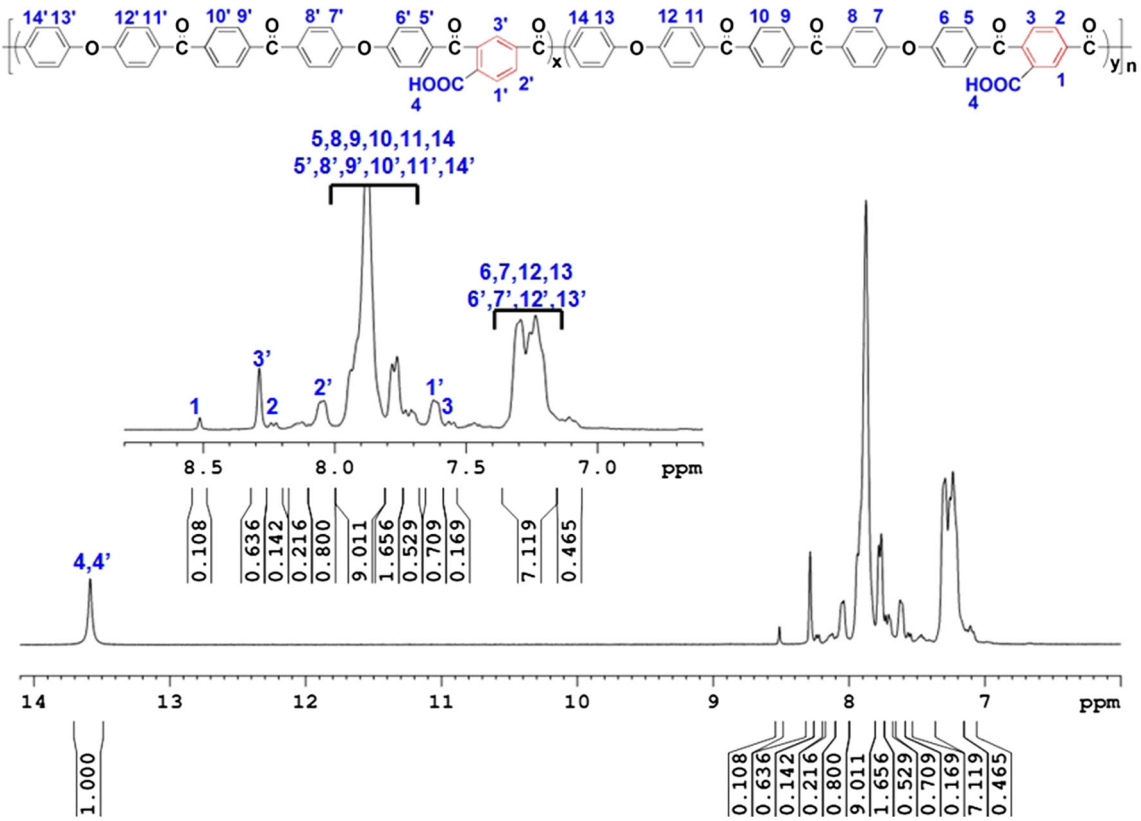

Fig. 1 ^{1}H NMR spectrum of PEKK with carboxylic acid pendant groups

increase too quickly for incorporation of base catalyst. So, in this study, only acid catalyst was used to catalyze the hydrolysis and condensation reactions of trimethoxysilane pendant groups of PEKK.

The preparation of PEKK–silica composite wet gel is described in Scheme 2. After adding water and acid catalyst, the methoxy groups on silicon were firstly hydrolyzed to silanols that subsequently condensed with each other or with other methoxy groups on silicon to form a cross-linked Si–O–Si network structure, causing the polymer solution to become viscous [41].

PEKK–silica composite aerogels with different densities were prepared by adjusting the concentration of PEKK with trimethoxysilane pendant groups in DMF (Table 1). Figure 3a shows the complex viscosities of the PEKK solutions at room temperature after adding water and acid catalyst, in which a continuous increase in the complex viscosities with time was observed. The evolution of

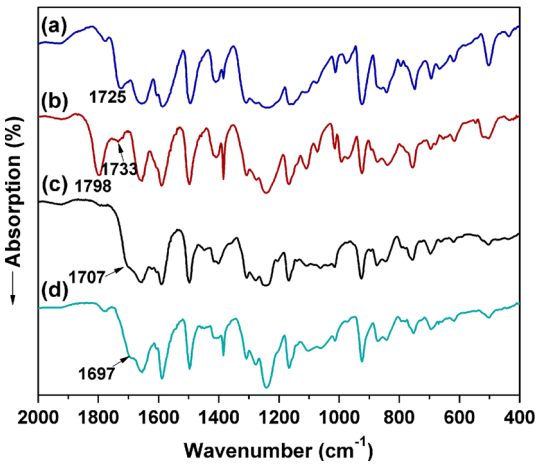

Fig. 2 *a* FTIR spectrum of PEKK with carboxylic acid pendant groups; *b* FTIR spectrum of PEKK with acyl chloride pendant groups; *c* FTIR spectrum of PEKK with trimethoxysilane pendant groups; *d* FTIR spectrum of the final PEKK–silica composite aerogel

storage modulus (G′) and loss modulus (G″) of the PEKK solutions as a function of time is also shown in Fig. 3b. The two curves crossed near the gelation point, beyond which the elastic property of the newly formed wet gel dominated over the viscous property of the fluid [42]. Accordingly, the gelation times of PEKK solutions with initial concentrations of 0.04, 0.05 and 0.06 g/mL were 52 ± 7, 30 ± 3 and 15 ± 2 min, respectively. Since higher content of trimethoxysilane pendant group contributed to higher cross-link density after the same reaction time, the complex viscosity at the same reaction time decreased and the gelation time increased with decreasing the initial solution concentration. Within a short time after adding HCl and water, the PEKK solutions can be cast as films or drawn into syringes. In order to observe shrinkage clearly and avoid absorbing water from atmosphere by DMF, the gelation was performed in sealed syringes (Fig. 4). As the condensation reaction proceeded, the PEKK–silica composite wet gel shrank and the solvent inside were expelled gradually. After 3-day aging, elastic and strong PEKK–silica composite wet gels were obtained.

The PEKK–silica composite wet gels were dried by freeze-drying from *tert*-butanol to obtain PEKK–silica composite aerogels. The hydrolysis and condensation reactions of trimethoxysilane pendant groups of PEKK afforded the cross-linked Si–O–Si network structure of the final PEKK–silica composite aerogel. Since the Si–O

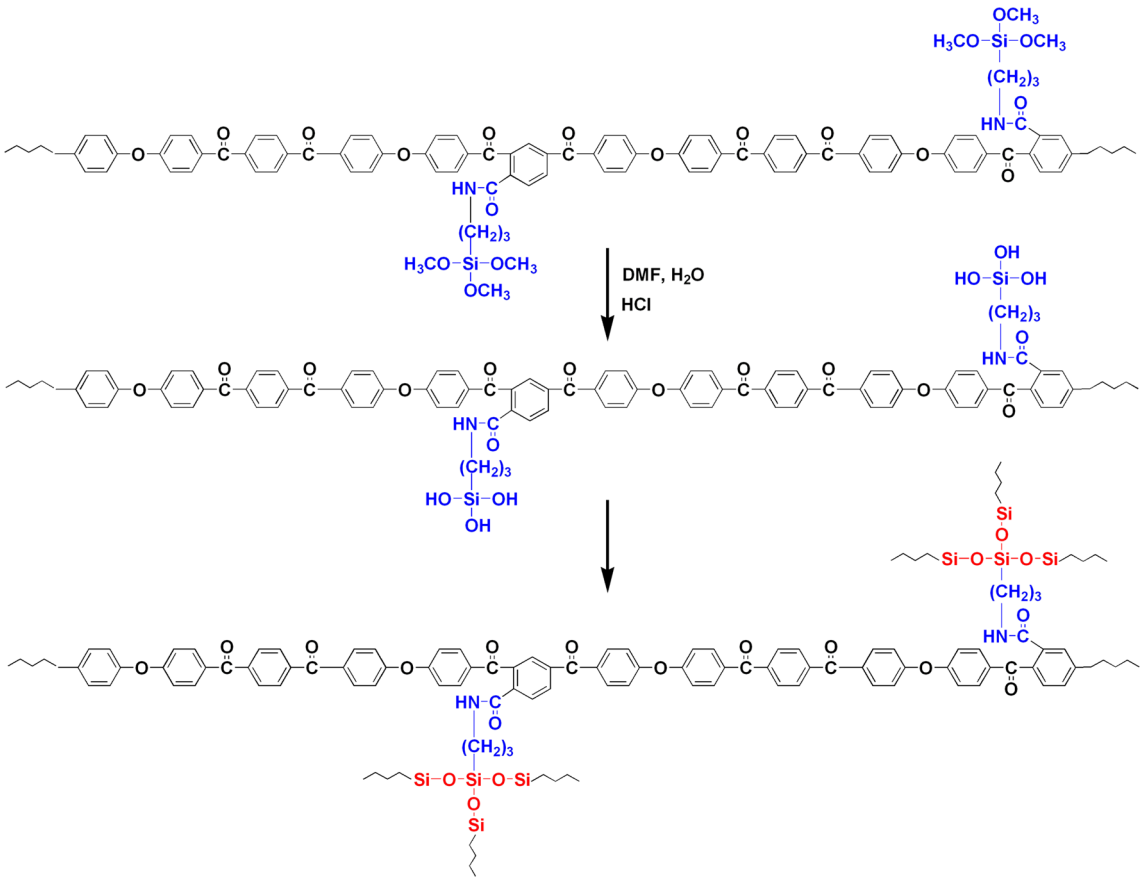

Scheme 2 Synthesis of PEKK–silica composite wet gel based on the trimethoxysilane pendant groups of PEKK

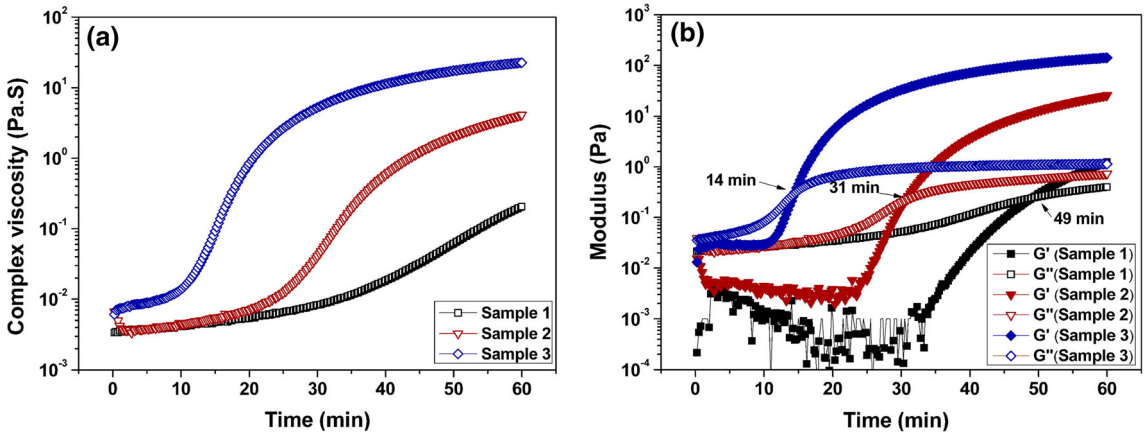

Fig. 3 **a** Evolution of complex viscosity versus time after adding HCl and water in the solution of PEKK with trimethoxysilane pendant groups; **b** evolution of storage modulus (G′) and loss modulus (G″) versus time after adding HCl and water in the solution of PEKK with trimethoxysilane pendant groups

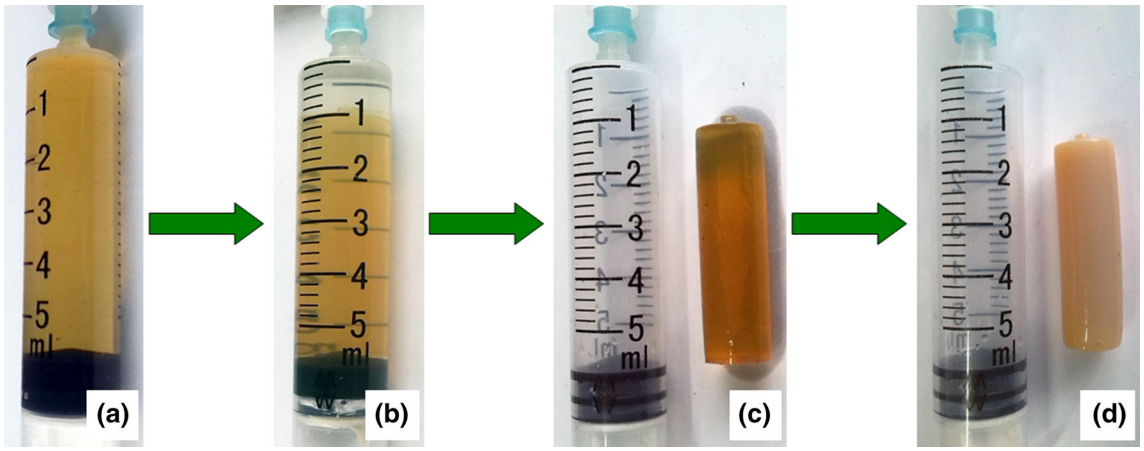

Fig. 4 Photograph of **a** Sample 1 before aging; **b** Sample 1 after three-day aging; **c** Sample 1 removed from the syringe; **d** Sample 1 after solvent exchange with *tert*-butanol

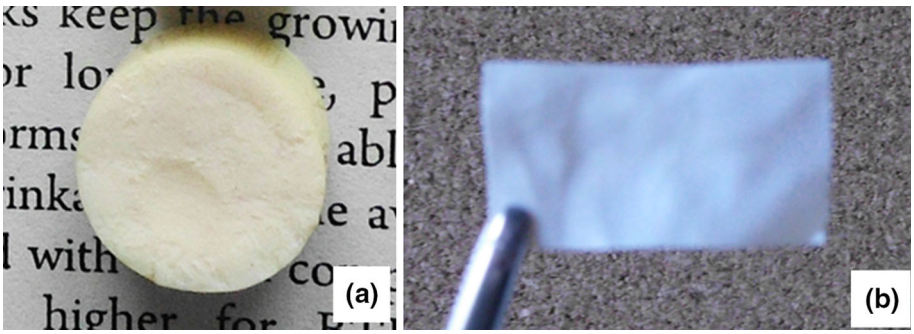

Fig. 5 Photographs of Sample 1 (**a** cylinder; **b** film with thickness of 0.32 mm)

stretch absorption peak (between 1000 and 1100 cm^{-1}) of $Si–O–CH_3$ overlapped with that of Si–O–Si, there was no significant difference in FTIR absorption peak position between the PEKK with trimethoxysilane pendant groups and the final PEKK–silica composite aerogel (Fig. 2). Figure 5 shows the photographs of Sample 1 after drying. Different from the wet gel which was red–brown, the resulting aerogel was grayish white. A probable reason for the difference in their colors was this: The wet gel was transparent, and the red–brown color was accumulated from the whole wet gel body and related to the thickness of the wet gel. If the wet gel was cut into thin slices, the color

was very light. On the contrary, the aerogel was opaque (even for sample with thickness of 0.32 mm, it was still opaque.). As a result, the light reflected on the surface of aerogel and had no relationship with the thickness of aerogel.

All samples did exhibit noticeable shrinkage (40–44 % in diameter) during aging, solvent exchange and drying, so the densities of the PEKK–silica composite aerogels were much larger than the corresponding initial solution concentrations (Table 1). Since more trimethoxysilane pendant groups contributed to PEKK–silica composite wet gel with higher cross-link density and strength, PEKK–silica composite aerogel prepared from higher initial solution concentration had higher shrinkage during aging but lower shrinkage during solvent exchange and freeze-drying.

Figure 6 shows the ^{29}Si solid-state NMR spectrum of Sample 2. When only one methoxy group on silicon participated in the condensation reaction (represented by T^1), the chemical shift of silicon was at −48 ppm; when two methoxy groups on silicon participated in the condensation reaction (represented by T^2), the chemical shift of silicon was at −56 ppm; when three methoxy groups on silicon participated in the condensation reaction (represented by T^3), the chemical shift of silicon was at −64 ppm [43, 44]. So, ^{29}Si solid-state NMR spectrum could be used to quantitatively measure the condensation degree of methoxy groups on silicon by comparing the intensities of T^1, T^2 and T^3. According to Fig. 6, the molar ratio of T^1:T^2:T^3 was 0.091:0.702:0.207. As a result, 70.5 % of the methoxy groups on silicon participated in the condensation reaction. So, although only HCl was used to catalyze the hydrolysis and condensation reactions of the trimethoxysilane pendant groups, most of methoxy on silicon still formed cross-linked Si–O–Si network.

The internal texture of the PEKK aerogels was observed by scanning electron microscopy (SEM). Figure 7 shows the SEM photographs of the PEKK–silica composite aerogels measured at magnifications of 25× and 100× K. The PEKK–silica composite aerogels had an interconnected fibrillar skeleton structure. With increase in the density, the fibrillar structure became denser and the pore size became smaller.

Porosity, as a percent of empty space, was calculated via $100 \times (1 - \rho_{bulk}/\rho_{skeletal})$, in which ρ_{bulk} and $\rho_{skeletal}$ were bulk density and skeletal density, respectively. Table 2 summarizes the relevant data, which were in the range of 71–86 % and showed a decrease trend with increase in the density of PEKK–silica composite aerogel.

The pore structure of PEKK–silica composite aerogels was also characterized by N_2 sorption measurement. As shown in Fig. 7, because of capillary condensation in mesopores, the volume of N_2 adsorbed increased significantly at high relative pressure ($P/P_0 > 0.8$). It should be also noted that N_2-sorption isotherms of Sample 2 and Sample 1 did not reach saturation. This was because they contained macropores that were too big to be detected by N_2 sorption experiment [45]. The total pore volume per gram of sample V_{Total} was either calculated by multiplying the highest adsorption point in the isotherm by 0.001547 or calculated from the relationship $V_{Total} = (1/\rho_{bulk}) - (1/\rho_{skeletal})$. In addition, $V_{1.7–300nm}$, the cumulative volume of pores with diameters in the range of 1.7–300 nm, is also given in Table 2. Notably, V_{Total} calculated from the relationship $V_{Total} = (1/\rho_{bulk}) - (1/\rho_{skeletal})$, V_{Total} calculated by multiplying the highest adsorption point in the isotherm by 0.001547 and $V_{1.7–300}$ nm were numerically close in the case of Sample 3. However, since N_2 sorption did not probe macropores [45], for the lower-density samples, V_{Total} calculated from the relationship $V_{Total} = (1/\rho_{bulk}) - (1/\rho_{skeletal})$ diverged from V_{Total} calculated by multiplying the highest adsorption point in the isotherm by 0.001547 and $V_{1.7–300}$ nm.

The pore size distribution could be calculated from the desorption branch of the N_2 isotherm through the Barrett–Joyner–Halenda (BJH) method [20, 21]. However, because Sample 1 and Sample 2 contained macropores that

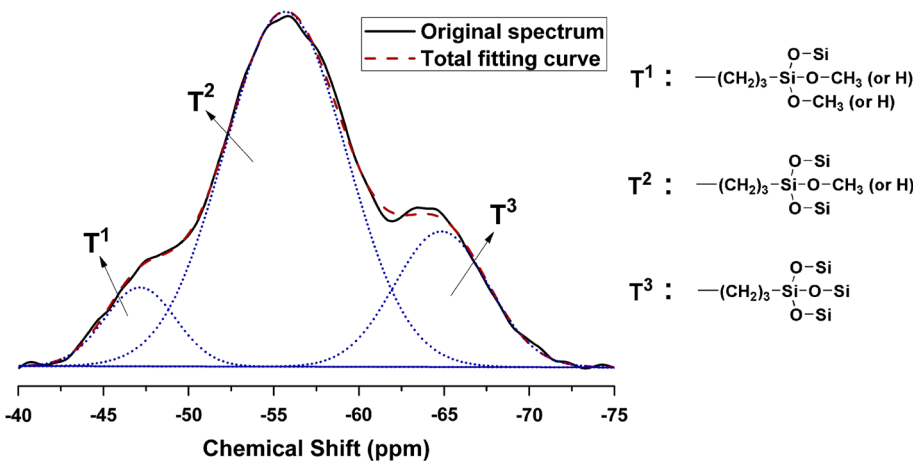

Fig. 6 ^{29}Si solid-state NMR spectrum of Sample 2

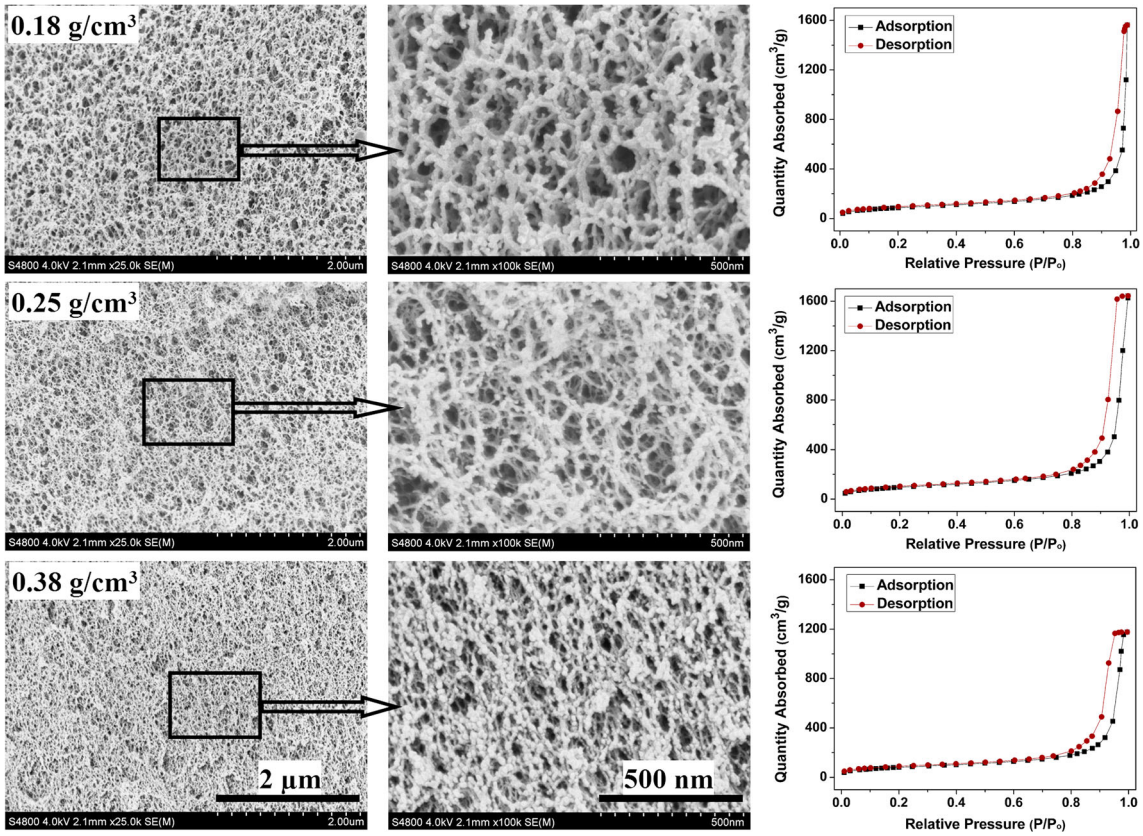

Fig. 7 SEM photographs and N_2 adsorption–desorption isotherms of the PEKK–silica composite aerogels with different densities

Table 2 Properties of the PEKK–silica composite aerogels

Sample	Porosity (%)[a]	BET surface area (m^2/g)	V_{Total} (cm^3/g)[b]	$V_{1.7–300nm}$ (cm^3/g)	Average pore diameter (nm)[c]	$T_{5wt\%}$ (°C)[d]	Thermal conductivity (W/m K)[e]
Sample 1	86	323	4.80 (2.39)	2.37	59.4	379	0.024
Sample 2	81	354	3.24 (2.54)	2.52	36.6	375	0.029
Sample 3	71	299	1.87 (1.82)	1.80	25.0	391	0.035

[a] Porosity was calculated via $100 \times (1 - \rho_{bulk}/\rho_{skeletal})$, where ρ_{bulk} and $\rho_{skeletal}$ were bulk density and skeletal density, respectively. The $\rho_{skeletal}$ of the PEKK aerogels was 1.32 g/cm^3

[b] V_{Total} was the total pore volume per gram of sample. For the first value, V_{Total} was calculated based on the relationship $V_{Total} = (1/\rho_{bulk}) - (1/\rho_{skeletal})$; for the value in bracket, V_{Total} was the highest adsorption point in the isotherm

[c] The average pore diameter was calculated via $4 \times V_{Total}/\sigma$, where V_{Total} was calculated based on the relationship $V_{Total} = (1/\rho_{bulk}) - (1/\rho_{skeletal})$

[d] 5 % weight loss temperature under air atmosphere

[e] Measured at room temperature

could not be detected by the N_2 sorption experiment, pore size distributions based on the BJH method did not express their true pore size distributions and were not given. However, the average pore diameters could be calculated via the $4 \times V_{Total}/\sigma$ method, where σ was surface area and V_{Total} was calculated from the relationship $V_{Total} = (1/\rho_{bulk}) - (1/\rho_{skeletal})$. The surface areas of PEKK–silica composite aerogels inferred from their N_2 adsorption branches by the Brunauer–Emmett–Teller (BET) method were in the range of 299–354 m^2/g. As shown in Table 2, the average pore diameters of the three samples were in the range of 25.0–59.4 nm, which were smaller than the mean free path of air molecules (~70 nm) and decreased with increasing the density of PEKK–silica composite aerogel.

To demonstrate the mechanical property of the PEKK–silica composite aerogels, the compression test was evaluated on the three samples. Prior to testing, the samples were polished to make sure that the top and bottom

surfaces were smooth and parallel. All of the three samples were compressed until the strain reached 80 %. Figure 8 shows the stress–strain curves with an insert magnifying the 0–20 % strain. Different from pure silica aerogel, the PEKK–silica composite aerogels did not shatter into fragment under compression. The compression stress–strain curves of PEKK–silica composite aerogels showed a short linear range followed by plastic deformation and inelastic hardening. Increasing the density of PEKK–silica composite aerogel, inelastic hardening occurred at lower strain.

The ambient thermal conductivities of PEKK–silica composite aerogels are tested and summarized in Table 2. The data were in the range of 0.024–0.035 W/m K and showed a decrease trend with decrease in the density of PEKK–silica composite aerogel. In conventional thermal insulation materials like foamed polymers or mineral wool or glass wool, heat is mainly transferred by the gas within pores [6]. So, a potential for further improving thermal insulation property can be realized by reducing the gas heat conduction. According to the above analysis, the average pore sizes of the PEKK–silica composite aerogels (ranging from 25.0 to 59.4 nm) were smaller than the mean free path of air molecules, facilitating the gas heat conduction in PEKK–silica composite aerogels to reduce [3]. As a result, the lowest thermal conductivity achieved (0.024 W/m K) was lower than the thermal conductivities of conventional thermal insulation materials such as mineral wool (0.034–0.045 W/m K), glass wool (0.031–0.045 W/m K), foam glass (0.038–0.050 W/m K) and expanded polystyrene (0.029–0.055 W/m K) [1].

For materials used for thermal insulation, thermal stability is a very important value. According to the results of thermogravimetric analysis (Table 2), the 5 % weight loss temperatures of PEKK–silica composite aerogels were in the range of 375–391 °C under air atmosphere. It is well-known that linear PEKK is a semicrystalline polymer and

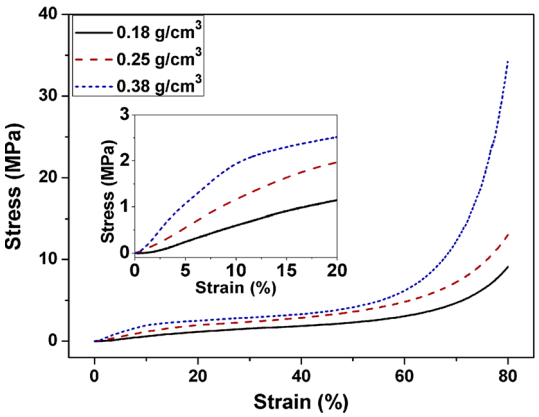

Fig. 8 Compressive stress–strain curves of PEKK–silica composite aerogels with different densities

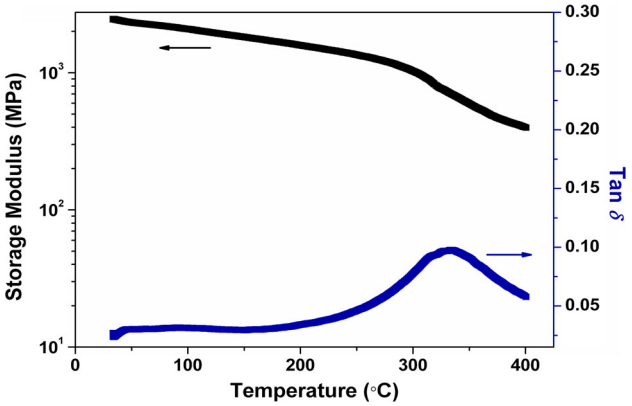

Fig. 9 DMTA result of the PEKK cross-linked by trimethoxysilane pendant groups under air atmosphere

has well-defined diffractions at 2θ values of 11°, 13° and 15° after annealing between 200 and 340 °C [36, 37]. In this study, we also evaporated the DMF solvent in PEKK–silica composite wet gel slowly at room temperature to get a dense cross-linked PEKK–silica composite film, which was then undertaken WXRD and DMTA measurements. No diffraction peak was found in the WXRD result of the cross-linked PEKK–silica composite film after being heated at 250 °C for 30 min under nitrogen atmosphere, indicating that the PEKK lost the crystallization ability after incorporating trimethoxysilane pendant groups and cross-linked Si–O–Si structure. However, the cross-linked PEKK still had a storage modulus as high as 1026 MPa at 300 °C (Fig. 9). Pore size of Sample 1 was bigger than that of the other two samples. In order to observe the change in pore structure of the PEKK–silica composite aerogel after being heated more clearly, SEM characterization was performed on Sample 1 heated at 250 °C for 30 min and 300 °C for 30 min. As shown in Fig. 10, even after being heated at 250 °C for 30 min in air, the pore structure of PEKK–silica composite was still intact.

4 Conclusion

In this study, PEKK–silica composite aerogel was prepared based on PEKK with trimethoxysilane pendant groups. The incorporation of trimethoxysilane pendant groups not only increased the solubility of semicrystalline PEKK, but also helped to form PEKK–silica composite wet gel with cross-linked Si–O–Si structure through their hydrolysis and condensation reactions. Due to the high reactivity of the trimethoxysilane pendant groups and the inherent flexibility of the $-(CH_2)_3-$ linkage linking the trimethoxysilane groups to PEKK main chain, most of methoxy groups on silicon participated in the condensation reaction. The resulting PEKK–silica composite aerogel consisted of

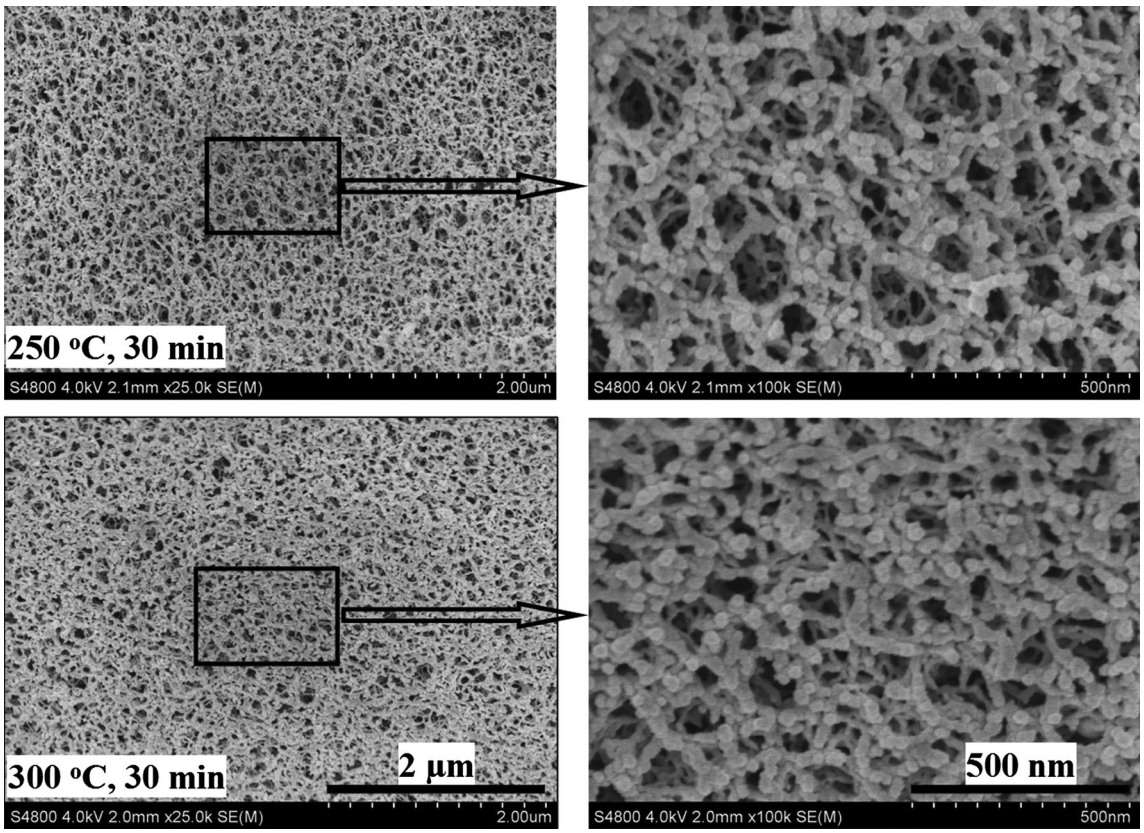

Fig. 10 SEM photographs of Sample 1 after being heated at 250 °C for 30 min and at 300 °C for 30 min under air atmosphere

polymer fibers tangled together, and its pore size and density could be adjusted simply by altering initial concentration of the PEKK with trimethoxysilane pendant groups. Highly cross-linked structure endowed the PEKK–silica composite aerogel with good thermal stability and mechanical strength. Furthermore, because of three-dimensional skeleton structure, low density and small pore size, it had low thermal conductivity. So, the prepared PEKK–silica composite aerogel could be considered as a new candidate for thermal insulation of building, aerospace, refrigerator, petrochemical pipelines and so on.

Acknowledgments This work was financially supported by National Natural Science Foundation of China (Grant No. 51403226) and Natural Science Foundation of Ningbo City, China (Grant No. 2014A610139).

References

1. Koebel M, Rigacci A, Achard P (2012) J Sol-Gel Sci Technol 63:315–339
2. Hüsing N, Schubert U (1998) Angew Chem Int Ed 37:22–45
3. Shi JJ, Lu LB, Guo WT, Zhang JY, Cao Y (2013) Carbohyd Polym 98:282–289
4. Luo YW, Ye CH (2012) Polymer 53:5699–5705
5. Li LC, Yalcin B, Nguyen BN, Meador MAB, Cakmak M (2009) ACS Appl Mater Interfaces 1:2491–2501
6. Koebel MM, Rigacci A, Achard P (2011) In: Aegerter MA, Leventis N, Koebel MM (eds) Aerogels handbook. Springer, New York
7. Pierre AC, Pajonk GM (2002) Chem Rev 102:4243–4265
8. Lu X, Arduini-Schuster MC, Kuhn J, Nilsson O, Fricke J, Pekala RW (1992) Science 255:971–972
9. Guo HQ, Meador MAB, McCorkle L, Quade DJ, Guo J, Hamilton B, Cakmak M, Sprow G (2011) ACS Appl Mater Interfaces 3:546–552
10. Cuce E, Cuce PM, Wood CJ, Riffat SB (2014) Renew Sustain Energ Rev 34:273–299
11. Kamiuto K, Miyamoto T, Saitoh S (1999) Appl Energ 62:113–123
12. Zhang G, Dass A, Rawashdeh AM, Thomas J, Counsil JA, Sotiriou-Leventis C, Fabrizio EF, Ilhan F, Vassilaras P, Scheiman DA, McCorkle L, Palczer A, Johnston JC, Meador MAB, Leventis N (2004) J Non-Cryst Solids 350:152–164
13. Woignier T, Phalippou J (1988) J Non-Cryst Solids 100:404–408
14. Zhao JJ, Duan YY, Wang XD, Wang BX (2012) Int J Heat Mass Transf 55:5196–5204
15. Duan YN, Jana SC, Lama B, Espe MP (2013) Langmuir 29:6156–6165
16. Maleki H, Durães L, Portugal A (2014) J Non-Cryst Solids 385:55–74
17. Mulik S, Sotiriou-Leventis C, Churu G, Lu HB, Leventis N (2008) Chem Mater 20:5035–5046
18. Lee JK, Gould GL, Rhine W (2009) J Sol-Gel Sci Technol 49:209–220

19. Tan C, Fung BM, Newman JK, Vu C (2001) Adv Mater 13:644–646
20. Leventis N, Sotiriou-Leventis C, Chandrasekaran N, Mulik S, Larimore ZJ, Lu HB, Churn G, Mang J (2010) Chem Mater 22:6692–6710
21. Leventis N, Chidambareswarapattar C, Mohite DP, Larimore ZJ, Lu HB, Sotiriou-Leventis C (2011) J Mater Chem 21:11981–11986
22. Ding BB, Cai J, Huang JC, Zhang LN, Chen Y, Shi XW, Du YM, Kuga S (2012) J Mater Chem 22:5801–5809
23. Yang J, Li SK, Yan LL, Liu JX, Wang FC (2010) Micropor Mesopor Mater 133:134–140
24. Pei XL, Zhai WT, Zheng WG (2014) Langmuir 30:13375–13383
25. Dai RY, Song CS, Zhong M, Xu L, Huang H (2007) J Jiangxi Normal Univ (Natural science) 31:518–522
26. Daniel C, Longo S, Ricciardi R, Reverchon E, Guerra G (2013) Macromol Rapid Commun 34:1194–1207
27. Daniel C, Vitillo JG, Fasano G, Guerra G (2011) ACS Appl Mater Interfaces 3:969–977
28. Peterson G, Cychosz KA, Thommes M, Hope-Weeks LJ (2012) Chem Commun 48:11754–11756
29. Figueroa-Gerstenmaier S, Daniel C, Milano G, Vitillo JG, Zavorotynska O, Spoto G, Guerra G (2010) Macromolecules 43:8594–8601
30. Bang A, Buback C, Sotiriou-Leventis C, Leventis N (2014) Chem Mater 26:6979–6993
31. Mahadik-Khanolkar S, Donthula S, Sotiriou-Leventis C, Leventis N (2014) Chem Mater 26:1303–1317
32. Schwan M, Ratke L (2013) J Mater Chem A 1:13462–13468
33. Yang X, Cranston ED (2014) Chem Mater 26:6016–6025
34. Williams JC, Meador MAB, McCorkle L, Mueller C, Wilmoth N (2014) Chem Mater 26:4163–4171
35. Meador MAB, McMillon E, Sandberg A, Barrios E, Wilmoth NG, Mueller CH, Miranda FA (2014) ACS Appl Mater Interfaces 6:6062–6068
36. Hsiap BS, Gardner KH, Cheng SZD (1994) J Polym Sci Polym Phys 32:2585–2594
37. Gardner KH, Hsiao BS, Matheson RR Jr, Wood BA (1992) Polymer 33:2483–2495
38. Son YG, Chun YS, Weiss RA (2004) Polym Eng Sci 44:541–547
39. Zolotukhin MG, Colquhoun HW, Sestiaa LG, Rueda DR, Flot D (2003) Macromolecules 36:4766–4771
40. Dorcheh AS, Abbasi MH (2008) J Mater Process Technol 199:10–26
41. Loyt DA, Shea KJ (1995) Chem Rev 95:1431–1442
42. Chidambareswarapattar C, McCarver PM, Luo HY, Lu HB, Sotiriou-Leventis C, Leventis N (2013) Chem Mater 25:3205–3224
43. Loy DA, Jamison GM, Baugher BM, Russick EM, Assink RA, Prabakar S, Shea KJ (1995) J Non-Cryst Solids 186:44–53
44. Komori Y, Nakashima H, Hayashi S, Sugahara Y (2005) J Non-Cryst Solids 351:97–103
45. Hua J, Han Y (2009) Chem Mater 21:2344–2348